17th Brazilian Congress of Thermal Sciences and Engineering
November 25th-28th, 2018, Águas de Lindóia, SP, Brazil

ENCIT-2018-0670
DIMENSIONING OF A COMBUSTION CHAMBER FOR MICROTURBINE BASED ON AUTOMOTIVE TURBOCHARGER

Talita Mitsue Onose Araujo Cunha
Ramon Eduardo Pereira Silva
State University of Maringá, Colombo Avenue, 5790, Zone 07
Federal University of Grande Dourados, Dourados/Itaum Highway, km 12
pg400934@uem.br
ramonsilva@ufgd.edu.br

Abstract. *Gas turbines are well known for their in industrial and propulsion application. However, they have gained prominence due to their increasing potential for versatile power generation. This is due to the increase of energy demand, as well as cogeneration and distributed generation (DG) applications. Moreover, microturbines have grown in use recently. Some of the advantages, which make the microturbines stand out, are related to their considerable low cost and simplicity if compared to other power systems. Even though microturbines have been researched in countries as the U.S.A., few studies on how to design microturbines with different arrangements are found in the Brazilian scenario. This work demonstrated the application of a methodology developed for the design of high power capacity gas turbines for the design and project of a combustion chamber of a microturbine derived from an automotive turbocharger. Furthermore, the steps of calculation, as well as the specifications defined for the combustor are presented. The final project of the liner is displayed and compared to the literature.*

Keywords: *Combustion chamber, design, project, microturbine.*

1. INTRODUCTION (TIMES NEW ROMAN, BOLD, SIZE 10)

The growing need for electricity demand has driven new technologies for power generation, with emphasis on the use of gas turbines and microturbines. In addition to its well established application in thermoelectric plants, they have been used in cogeneration and distributed generation plants. Gas turbines are thermal machines that use the Brayton cycle as their working principle.

In this cycle, fuel energy is converted, by combustion with air, into mechanical energy or electricity. The basic components are the compressor, combustion chamber and gas turbine (CONRADO, 2002). Such machinery also has benefits such as: relatively low investment cost compared to other systems, smaller area used for the same power generation, low weight-to-power ratio, system simplicity and diversification of components (GOMES, 2001).

Therefore, the study of such equipment and the development of different arrangements of these is paramount. This can be achieved by the project and designing of turbines, mainly microturbines starting from components already available in the market. Thus, automotive turbochargers can be used as a basis for combustion chamber designs and gas microturbine assembly, reducing production costs.

2. COMBUSTION CHAMBER

The combustion chamber is divided into three main zones: primary zone, secondary zone and dilution zone. Combustion occurs in the primary zone and it is completed in the secondary zone. In order to overcome the losses generated by chemical dissociation of the combustion products, quantities of air are added in the secondary zone. On the other hand, in the dilution zone, unused air in the combustion reaction, and hot gases mix so that a reduction to an acceptable temperature of these gases at the entrance of the turbine takes place (CONRADO, 2002).

Flame stability in combustion chambers occurs by recirculation of the hot combustion gases. One of the biggest challenges is the adequacy of airflow in the primary zone, due to the adequacy of air flow, fuel ignition and flame discontinuity. As a solution, the secondary zone was created, which function is to allow the entrance of air needed for complete combustion. After combustion, to further distribute the heat and homogenize the temperature, the remaining air from the compressor is added to the dilution zone (MELCONIAN and MODAK, 1985). Figure 1 shows the combustion chamber with its zones.

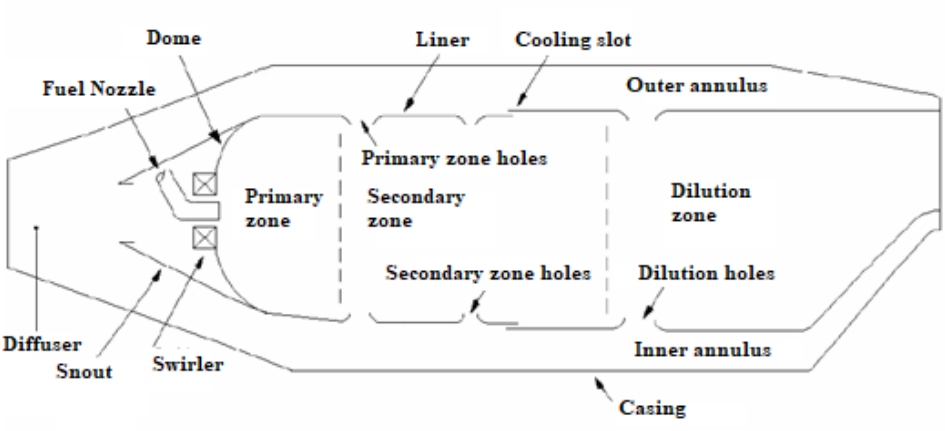

Figure 1 - Basic configuration of a combustion chamber.

Source: (Adapted from SILVA, 2006).

In order to ensure complete combustion, it is necessary to adjust the temperature increase in the chamber, as well as to operate with air / fuel ratio within the limits of flammability. Although ideal, the equivalence ratio of 0,8 for the primary zone produces NO_x emissions. In order to reduce them, the typical value of 0.6 is used (CARVALHO JUNIOR and LACAVA, 2003).

Another important factor is the type of air flow admitted in the combustion chamber, which is divided into: direct flow and reverse flow. In the direct flow, the flow has the same direction from the compressor to the turbine. Already in the reverse flow, the flow has its direction changed in the combustion chamber, which allows the concentric positioning of the combustor with the turbine and compressor. This also provides shortening of the shaft.

Table 1 – Compressor performance parameters

Parameter	Symbol	Value			Unit
Rotation		57	68	77	krpm
Isentropic efficiency	η_{comp}	77	76	72	%
Compression ratio	PR	2,5	3,5	4,5	
Total outlet pressure	P2	253312	354637	455962	Pa
Outlet temperature	T2	399,55	449,77	500,44	K
Mass airflow rate	mar	718,1877	831,586	982,7831	g/s
Mass fuel rate	mcomb	8,76	9,34	10,08	g/s

3. MICROTURBINE

The project was based on the methods presented by MELCONIAN and MODAK (1985) and LEFEBVRE and BALLAL, (2010), apud SILVA (2015) for combustors of large gas turbines operating with hydrocarbons. Related to this, in the study a microturbine is considered, this being composed by the adaptation of an automotive turbocharger Garrett GT5533R, also called GT55R

In this model both compressor and turbine are single stage centrifugal. The choice of reverse flow combustion chamber makes it possible to use the turbocharger shaft itself. The project was initiated by defining the requirements for the operating conditions and obtaining the thermodynamic data from the software Gasturb®, by the data found in the chosen efficiency curve of the compressor performance map given the rotations of 57 krpm, 68 krpm and 77 krpm (Table 1). In order to obtain such data, the thermodynamic conditions established by ISO 2314: 2009 and API 616: 2011 were considered, in which Tamb = 298.15 K and Pamb = 101.325 kPa, in addition to the expansion up to atmospheric pressure.

Table 2 – Compressor performance parameters

Parameter	Symbol	Value			Unit
Rotation		57	68	77	krpm
Isentropic efficiency	η_{comp}	77	76	72	%
Compression ratio	PR	2,5	3,5	4,5	
Total outlet pressure	P2	253312	354637	455962	Pa
Outlet temperature	T2	399,55	449,77	500,44	K
Mass airflow rate	mar	718,1877	831,586	982,7831	g/s
Mass fuel rate	mcomb	8,76	9,34	10,08	g/s

4. COMBUSTION CHAMBER DESIGN

4.1. Reference areas and diameters

The reference area serves as the basis for the other calculations of the dimensions of the chamber, since it is the cross-section of the carcass. The reference diameter is then formulated relative to this area. From the aerodynamic point of view, as well as based on MELCONIAN and MODAK (1985) and exemplified by SILVA, (2015), the reference area can be obtained as a function of pressure loss. This pressure loss, as presented by LEFEBVRE, (1983), apud CONRADO, (2002) and results obtained for reference area and diameter, calculated by equation 1 are shown in Table 2.

Table 3 - Pressure drop factor and reference dimensions calculated.

Rotation (krpm)	$\Delta P_{3\text{-}4}/q_{ref}$	A_{ref} (m^2)	D_{ref} (m)
57	37	0,015798	0,141827
68	37	0,013850	0,132794
77	37	0,013416	0,130696

$$A_{ref,aer} = \left[143{,}5.\left(\frac{\dot{m_{ar}}\sqrt{T2}}{P_2}\right)^2.\left(\frac{\Delta P_{2-3}}{q_{ref}}\right).\left(\frac{\Delta P_{2-3}}{P_2}\right)^{-1}\right]^{0,5} \quad (1)$$

On the other hand, the flame burning velocity method demonstrated by Lefebvre (1983), is based on the main operation parameters: pressure, temperature and mass flow. In addition, it correlates these parameters with a dimensionless parameter In order to obtain the best efficiency, the value of $73x10^6$ was assumed for θ as suggested by Melconian and Moldak (1985).

$$\theta_\eta = \frac{P_2^{1,75}.A_{ref,vq}.D_{ref,vq}^{0,75}.exp\left(\frac{T_2}{b}\right)}{\dot{m_{ar}}} \quad (2)$$

However, if compared both results computed from the aerodynamic considerations and burning flame method, this last one does not fit in with the criteria required by the other. Therefore, the chosen values for reference parameters were A_{ref}=0,016 and D_{ref}=0,150.

4.2. Airflow distribution and cooling film

After computing the reference parameter, the next step is to determine the airflow and length of the combustion zones. The airflow used for cooling has its proportion calculated from equation 3, demonstrated by ODGERS (1980) and applied by SILVA (2015).

$$\frac{\dot{m_{refri}}}{\dot{m_{ar}}} = 0{,}1.T_2 - 30 \tag{3}$$

For the remaining zones, the equivalence ratio, is used to compute their values. In the primary zone, as argued by Lefebvre and Ballal (2010), the equivalence ratio must not be less than ϕ_{zs}=0,8, in order to minimize pollutants such as carbon monoxide (CO) among the exhaust gases. Moreover, it also relates to the requirement of flame temperature of 1660K to preserve a complete combustion. The results for airflow distribution are shown in table 3.

Table 4 - Airflow distribution.

Parameter	Airflow (%)		
Rotation (krpm)	57	68	77
Cooling	9,955	14,977	20,044
Primary zone	30	30	30
Secondary zone	45	45	32,5
Dilution zone	15,045	10,023	17,456

4.3. Combustion zone lengths

According to Melconian and Modak (1985) that the length of the primary zone should be within the range of 2/3 and 3/4 of Dref. This second value promotes a higher combustion efficiency. On the other hand, the proportion for the secondary zone is half of the diameter of the flame tube, whereas the total length of the flame tube considers the transverse quality of the temperature distribution, for preservation of the turbine vanes purposes. The dilution zone length is the subtraction of the primary and secondary zone length from the total length. The results for the flame tube length and its zones' length is shown in table 4.

Table 5 - Combustor lengths.

Primary zone (m)	Secondary zone (m)	Dilution zone (m)	Total (m)
0,098	0,065	0,11	0,271

4.4. Recirculation zone

In general, the design of the diffuser, which is responsable for pressure dropping by the airflow throughout the combustor, is determined according to dimensioning restrictions (CONRADO, 2002). Due to the fact that this Project aims the design of a microtubine with dimensioning restrictions and uniform airflow, the design of the diffuser can be dismissed.

However, a recirculation zone inside the primary zone, where the fuel is injected is needed to stabilize the flame. This region is computed by designing the swirler obtained frm equation (4).

$$\frac{\Delta P_{sw}}{q_{ref}} = K_{sw}.\left[\left(\frac{A_{ref}}{A_{sw}}\right)^2.sec^2\beta_{sw} - \left(\frac{A_{ref}}{A_{tc}}\right)^2\right].\left(\frac{\dot{m_{sw}}}{\dot{m_{ar}}}\right)^2 \tag{4}$$

Where, $\frac{\Delta P_{sw}}{q_{ref}}$ is the pressure drop on the swirler of 3-4% of P3, Ksw is the coeficiente for the blades (K=1.30 for straight blades) and the blade angle β_{sw} varies from 45 to 70. The swirl number gives the insity of the flow rate on the recirculation zone and it is set at 0.6 (Equation 5). The recirculation parameters are demonstrated in table 5.

$$S_n = \left\{\left(\frac{2}{3}\right).\left[\frac{1-\left(\frac{D_{int,sw}}{D_{sw}}\right)^3}{1-\left(\frac{D_{int,sw}}{D_{sw}}\right)^2}\right].tan\,\alpha_{sw}\right\} \tag{5}$$

Table 6 - Recirculation zone parameters.

Parameter	Value
Swirler outer diameter (m)	0,035
Swirler inner diameter (m)	0,015
8 thin straight blades (thickness=0,001m)	K=1.30
Recirculation zone length (m)	0,07
Angle of dome (m)	78
Length of dome (m)	0,011

4.5. Gas temperature profile in the combustion chamber

The main purpose of determining the gas temperature profile throughout the combustor is to verify the need for cooling inside the flame tube. The aim of this calculation is to find the higher temperature spots at the flame tube surface. In order to compute these temperature points, the computation of these temperatures was based on the methodology argued by Melconian and Modak (1985) and demonstrated by Silva (2015), which uses the combustion efficiency. In this methodology the recirculation zone temperature points are found from equations 6 and 7.

$$T_{fin,zr} = T_2 + \eta_{zr}.\Delta T_{\phi=1} \tag{6}$$

$$\eta_{zr} = 0{,}56 + 0{,}44.\tanh[1{,}5475.10^{-3}.(T_2 + 108.lnp_2 - 1863)] \tag{7}$$

Where, ηzr is the combustion efficiency for this zone and ΔTϕ=1 is the temperature variation of the adiabatic flame in the stoichiometric ratio. Analogously, for the primary zone equations 8 and 9 are applied.

$$T_{fin,zp} = T_2 + \eta_{zp}.\Delta T_{\phi_{zp}} \tag{8}$$

$$\eta_{zp} = 0{,}71 + 0{,}29.\tanh[1{,}5475.10^{-3}.(T_2 + 108.lnp_2 - 1863)] \tag{9}$$

As the secondary zone aims to complete the combustion, hence its efficiency is assumed to be 100% and its outlet temperature is computed from equation 10, likewise the temperature for the dilution zone is computed from equation 11.

$$T_{fin,zs} = T_2 + \eta_{zs}.\Delta T_{\phi_{zs}} \tag{10}$$

$$T_{fin,zd} = T_2 + \eta_{zd}.\Delta T_{\phi_{zd}} \tag{11}$$

The inlet temperature for the recirculation zone and primary zone are assumed the same as both inlets coincide. Moreover, for the remaining zones the outlet temperature of each zone is assumed to be the inlet temperature of the next zone. The results for the gas temperature profile for each zone is shown in table 6 and figure 2.

Table 7 - Gas temperature profile for each falme tube zone

Rotation (krpm)	Recirculation zone (K)	Primary zone (K)	Secondary zone (K)	Dilution zone (K)
57	1004,164	1280,288	2066,300	921,900
68	1122,194	1163,926	2102,300	966,400
77	1232,228	1171,627	2138,800	1011,700

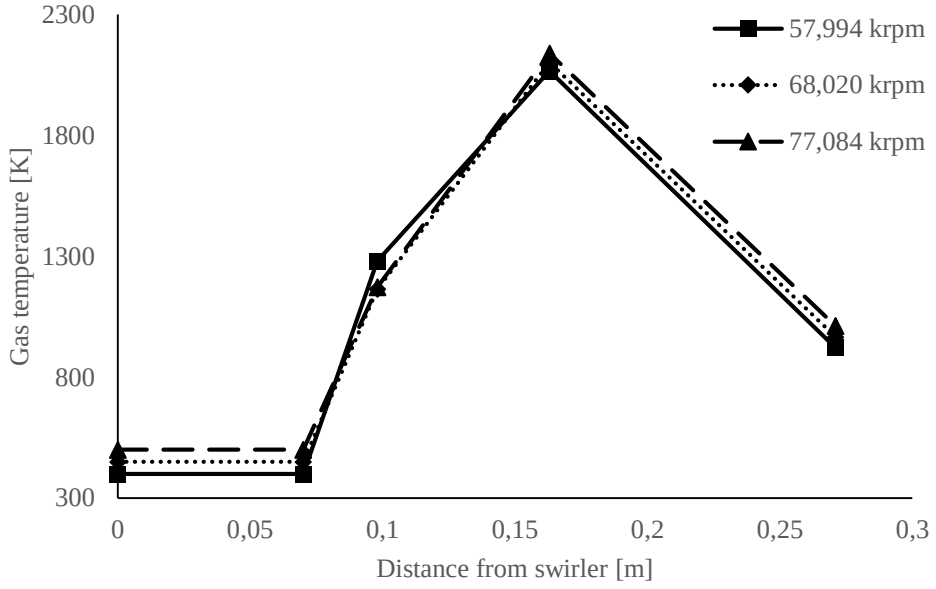

Figure 2 - Gas temperature profile.

4.6. Heat transfer to wall

Heat transfer to wall analysis in a combustor is used to identify and verify if the temperatures exceed its materials' limitations, according to the method defined by Lefebvre and Ballal (2010) and Gosselin et al. (1999). Therefore, once known the temperatures, if needed a cooling system is designed to keep surface structural integrity (NAVIA, 2010; SILVA;2015). For the sake of this analysis the liner is considered a cylinder with an internal flow of hot gases and external cooling airflow in the annulus region between the tube and its casing. The liner is heated by the radiation and convection of the hot gases and cooled by the radiation to the casing, as well as the convection to the annulus air. Due to the tube's very low thickness, the thermal resistance of the flame is neglected. Hence, the basic modeling for heat transfer is given as follows:

$$(R_1 + C_1) = (R_2 + C_2) = K_{1-2} \tag{12}$$

Where, R_1 and C_1 represent the internal radiation and convection, whereas R_2 and C_2 represent the external radiation and convection.

$$R_1 = 0{,}5.\sigma_{SB}.(1+\varepsilon_W).\varepsilon_g.T_g^{1,5}.(T_g^{2,5} - T_W^{2,5}) \tag{13}$$

$$C_1 = 0{,}020.\frac{k_g}{D_{tc}^{0,2}}.\left(\frac{\dot{m}_g}{A_{tc}.\mu_g}\right)^{0,8}.(T_g - T_{W1}) \tag{14}$$

$$R_2 = 0{,}6\sigma_{SB}(T_w^4 - T_2^4) \tag{15}$$

$$C_2 = 0{,}020.\frac{k_a}{D_{an}^{0,2}}.\left(\frac{\dot{m}_{an}}{A_{an}.\mu_{an}}\right)^{0,8}.(T_{W2} - T_2) \tag{16}$$

$$\varepsilon_g = 1 - \exp[-0{,}286.L_u.p_3.(f_{co}.0{,}9l_b)^{0,5}.T_g^{-1,5} \tag{17}$$

Where ε_g is the gas emissivity given by equation 17, D_{an} is the diameter of the annulus region and μ_{an} is the gas viscosity.

The combustion material considered was the steel, hence the equation 15 was used for external radiation (LEFEBVRE and BALLAL, 2010). Wall temperatures for each zone in the most critical project scenario, which is at the rotation of 77 krpm, were computed after an iterative approach as are shown in table 7.

Table 8 - Wall temperature for each flame tube zone

Zone	Recirculation	Primary	Secondary	Dilution
Temperature (K)	569	599	960	737

From table 7 it is noticeable that the highest temperature is found in the secondary zone with a value of 960K which is proportional to the temperature variation of this zone, also the highest of all for this project. This is linked to the fact that the highest airflow percentage is insert in as well as the combustion is completed takes place in this zone. According to Gosselin et al. (1999) and demonstrated by Silva (2015), the accuracy of this method lies around ± 100 K for the primary zone and ± 30 K. Therefore, the wall temperatures calculated do not compromise the material's structural integrity, no cooling slots are need and all the cooling air are to enter the inner side of the flame tube through admission holes at the end of the dilution zone.

4.7. Admission holes

An iterative method that considers the airflow rate for each zone is applied in order to find the optimal diameter of the air admission holes in the inner flame tube (LEFEBVRE e BALLAL, 2010). It consists of the following steps:

Step 1) Calculation of the bleed ratio, which is the ratio between the total hole airflow rate and the annulus airflow rate of each zone (equation 18).

$$\beta_h = \frac{\dot{m_{h,t}}}{\dot{m_{an}}} \tag{18}$$

Step 2) Estimate an initial value for the discharge coeficiente C_d.

Step 3) Calculate the total hole área from equation 19, considering that the pressure drop through the hole is $\Delta P_{tc}/P_2$= 6%.

$$\frac{\Delta P_{tc}}{P_2} = \frac{(143{,}5\ (\dot{m_{h,t}})^2 . T_2)}{P_2^2 . C_{d,h}^2 . A_{h,t}} \tag{19}$$

Step 4) Determine the area ratio αh (equation 20), by the ratio between the total hole área and the annulus área, as well as its relation to the bleed ratio β_h (Equação 21).

$$\alpha_h = \frac{A_h}{A_{an}} \tag{20}$$

$$\mu_h = \frac{\beta_h}{\alpha_h} \tag{21}$$

Step 5) Compute the pressure loss factor K from equation 22, where the momentum loss factor is δ=0,8 for plain holes and δ=0,6 for complex holes, (plain holes factor was assumed in this design).

$$K = 1 = \delta . \left\{ 2.\mu^2 + \left[4.\mu^4 + \left(\frac{\mu^2}{\delta^2} \right) . (4.\beta - \beta^2) \right]^{0,5} \right\} \tag{22}$$

Step 6) Use the value calculated for K to find the new value for C_d that satisfy equation 23.

$$C_{d,h} = \frac{(K-1)}{\delta [4K^2 - K.(2-\beta)^2]^{0,5}} \tag{23}$$

This process is sttoped once the values for discharge coefficient converge and the hole área is obtained. From this point the quantity of holes and rows of each zone are computed as shwon is table 8. The final design is shwon in figure 3.

Table 9 - Dimensions of admission holes

Zone	Number of holes	Diameter (mm)	x (mm)
Primary zone	20	9	0,070
Secondary zone	10	14	0,098
Dilution zone	15	8	0,163
Refrigeration zone	30	6	0,230

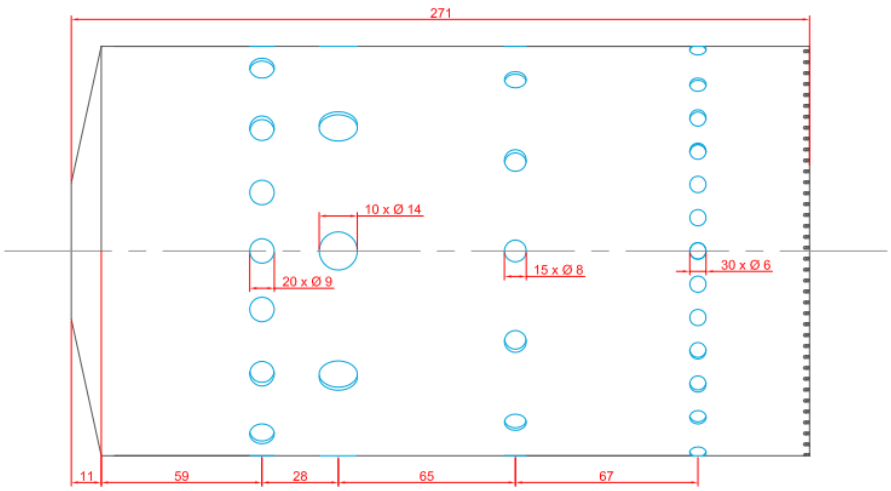

Figure 3 - flame tube geometry.

5. CONCLUSION

This work demonstrated that the methodology presented by Lefebvre and Ballal (2010) and Melconian & Modak (1985), firstly developed for large gas turbines may also be applied for the design of microturbines.

The use of a turbocharger eases the project and assembly of the microturbine. In addition, the use of methane as fuel led to large adiabatic flame temperature variations, which resulted in the highest temperatures in the secondary zone, as it was set as the combustion completion zone. Another characteristic of this microturbine is that it proposes lower temperatures at the turbine inlet than usual, which rules out the need for cooling slots while simplifying the machining process and lower costs.

6. REFERENCES

CARVALHO JUNIOR, João de Andrade de; MCQUAY, Mardson Queiroz. **Princípios de Combustão Aplicada.** Florianópolis: Editora da Ufsc, 2007.

CONRADO, Ana Costa. **Metodologia para projeto de câmara de combustão de turbina a gás.** 2002. 155 f. TCC (Graduação) - Curso de Engenharia Mecânica, Centro Técnico Aeroespacial, Ita - Instituto Tecnológico de Aeronáutica, São José dos Campos, 2002. Cap. 6.

GARRETT. **Turbocharger Guide.** 2004. Disponível em: <https://www.rbracing-rsr.com/downloads/Garrett_Cat 9 04.pdf>. Acesso em: 30 out. 2016.

GOMES, Eli Eber Batista et al. Aspectos econômicos e ambientais da aplicação de microturbinas a gás natural na geração distribuída. **Artigo). Escola Federal de Engenharia de Itajubá (EFEI). Itajubá**, 2001.

GOSSELIN, P.; DE CHAMPLAIN, A., KRETSCHMER, D. **Prediction of wall heat transfer for a gas turbine combustor.** Proceedings of The Institution of Mechanical Engineers Part A: Journal of Power and Energy.1999. n. 213 p 169-180.

LACAVA, Pedro Teixeira. **CAPÍTULO 4: PROJETO BÁSICO DE CÂMARA DE COMBUSTÃO:** São José dos Campos: Instituto Tecnológico de Aeronáutica, 2009. 60 slides, color.

LEFEBVRE A.H., **Gas turbine combustion.** Hemisphere, Washington DC, 1983.

LEFEBVRE, H.; BALLAL, D.R,. **Gas turbine combustion:** alternative fuels and emissions**.** England: CTCPress, 2010, 3th ed. 590 p.

MELCONIAN, J.O; MODAK, A.T. Combustor design. In: SAWYER, J.W. (Ed.) **Sawyer's gas turbine engineering handbook design**. Volume 1, Theory and design. 3. Ed. Connecticut: Turbomachinery International Publications, 1985. V.1, Chapter. 5 p 5-1-5-62.

NAVIA J. A. N. **Preliminary Design Methodology for Multi Fuel Gas Turbine Combustors**. 2010. 152 f. Dissertação (Mestrado em Engenharia Aeronáutica e Mecânica) – Instituto Tecnológico de Aeronáutica, São José dos Campos SP.

ODGERS, J. **Gas turbines fuels and their influence on combustion**. Abacus Press UK, 1986.

SILVA, H.M., **Procedimento para projeto de câmaras anulares de turbinas a gás.** 2006.74f. Trabalho de Conclusão de Curso (Graduação em Engenharia Aeronáutica) – Instituto Tecnológico de Aeronáutica, São José dos Campos.

SILVA, Ramón Eduardo Pereira. **PROJETO, CONSTRUÇÃO E ENSAIO DE UMA CÂMARA DE COMBUSTÃO DE MICROTURBINA OPERANDO COM ETANOL Ramón.** 2015. 180 f. Tese (Doutorado) - Curso de Engenharia Aeronáutica e Mecânica, Aerodinâmica, Propulsão e Energia, Istituto Tecnológico de Aeronáutica, São José dos Campos, 2015.

7. RESPONSIBILITY NOTICE

The authors are the only responsible for the printed material included in this paper.